Phytopathologia Mediterranea (2018), 57, 2, 296–306
DOI: 10.14601/Phytopathol_Mediterr-21881

RESEARCH PAPERS

Detection of *Erwinia amylovora* in pear leaves using a combined approach by hyperspectral reflectance and nuclear magnetic resonance spectroscopy

Antonino RIZZUTI[1,2], Luis Manuel AGUILERA-SÁEZ[1], Franco SANTORO[3], Franco VALENTINI[3], Stefania GUALANO[3], Anna Maria D'ONGHIA[3], Vito GALLO[1,2], Piero MASTRORILLI[1,2] and Mario LATRONICO[1,2]

[1] Dipartimento di Ingegneria Civile, Ambientale, del Territorio, Edile e di Chimica, Politecnico di Bari, Via Orabona, 4, I-70125, Bari, Italy
[2] Innovative Solutions S.r.l. – Spin off company of Politecnico di Bari, zona H, 150/B, I-70015, Noci (BA), Italy
[3] CIHEAM - Istituto Agronomico Mediterraneo di Bari, Via Ceglie, 9, I-70010, Valenzano (BA), Italy

Summary. *Erwinia amylovora* infections on pear leaves were studied using nuclear magnetic resonance and hyperspectral reflectance spectroscopies. Inoculated pear plants under controlled conditions were used for comparing *Erwinia amylovora* infected leaves with those infected by *Pseudomonas syringae* pv. *syringae* or non-infected controls. Hyperspectral reflectance-NMR covariance analysis allowed the transfer of metabolome information obtained by NMR to hyperspectral reflectance bands through a knowledge transfer approach. At 20 d after *Erwinia amylovora* inoculation, correlation was found between the NMR signal at 1.16 ppm (attributed to the methyl group of a fucosyl-containing polysaccharide, identified as a specific metabolite from *Erwinia amylovora*) and a hyperspectral reflectance band centred at 1400 nm. At 50 d after inoculation the same marker metabolite was correlated to hyperspectral reflectance bands centred at 850 nm and 1050 nm. These methods allow maps to be developed which represent the specific infection status of pear plants, and could facilitate development of simple, fast and affordable hyperspectral reflectance-based devices for the detection of *Erwinia amylovora* infections on pear leaves.

Key words: *Pyrus communis*, metabolome, spectroscopic analysis, fire blight, covariance analysis.

Introduction

Fire blight, caused by *Erwinia amylovora* (*Ea*), is one of the most important bacterial diseases that affects production of pears, apples and other rosaceous crops (Bonn and van der Zwet, 2000). Since 1975, *Ea* has been recognized as a harmful quarantine pest, according to the A2 list of the European and Mediterranean Plant Protection Organization (EPPO).

Erwinia amylovora can survive as endophytes or epiphytes for variable periods, depending on environmental factors (Thomson, 2000). The development of symptoms on host plants is related to seasonal growth of the hosts and climatic conditions, starting in spring with production of primary inoculum and infection of flowers, continuing in summer with infection of shoots and fruits, and ending in autumn with the development of cankers. The pathogen is apparently quiescent throughout host dormant periods (van der Zwet and Beer, 1995). Leaf symptoms induced by *Ea* are either necrotic patches, which develop on the margins of leaf blades, or blackening of petioles and leaf midribs, depending on the mode of infection (Thomson, 2000).

Since the symptoms of fire blight generated by *Ea* may be confused with those caused by other bacteria such as *Pseudomonas syringae* pv. s*yringae* (*Pss*), treatments to eradicate the disease could be ineffective because of a wrong diagnoses. Currently, the most ef-

Corresponding author: M. Latronico
E-mail: mario.latronico@poliba.it

ISSN (print): 0031-9465
ISSN (online): 1593-2095
www.fupress.com/pm

ficient strategies for management of disease caused by *Ea* are a combination of stringent quarantine measures, sanitation, appropriate agronomic practices, chemical or biological treatments, along with vigilant and regular crop inspections.

The use of predictive models, which correlate the development of disease with pedoclimatic parameters, are useful to warn technicians and farmers of the incipient pest risk in pear trees and apple orchards. These are especially useful during flowering and post-flowering periods, when diffusion of the bacterium is most probable (Jacquart-Romon and Paulin, 1991; Billing, 2000). However, large scale detection of the first symptoms is not always easy to attain, due to the large numbers of trees to be inspected. Moreover, pathogen detection in asymptomatic plants is also difficult, and depends on favourable climatic conditions and susceptibility of the host plants and cultivars.

Two ways to achieve early detection of the presence of *Ea* are the use of the metabolomics and proximal sensing approaches. Metabolomics aims to measure the global, dynamic metabolic response of living systems to biological stimuli, and provides information on a wide range of detectable chemical compounds contained in food products (Nicholson and Lindon, 2008). Metabolomic studies are often based on Nuclear Magnetic Resonance (NMR) spectroscopy, integrated with multivariate statistical methods (Ali *et al*., 2011; Bevilacqua *et al*., 2012; Ferrara *et al*., 2013, 2014; Longobardi *et al*., 2013; Gallo *et al*., 2014; Rizzuti *et al*., 2015). NMR spectroscopy has been used for detection of symptomatic and asymptomatic plant diseases (Sankaran *et al*., 2010), as well as for investigations of metabolites acting as signal compounds and protecting agents produced during host plant resistance processes (Leiss *et al*., 2011). Other studies have focused on the identification of metabolic pathways connected with the defence responses, to *Esca* disease of *Vitis vinifera* (Lima *et al*., 2010) and phytoplasma in *Catharanthus roseus* (Choi *et al*., 2004).

As a proximal sensing technique, Hyperspectral Reflectance (HR) has been used for the detection of biotic and abiotic stresses in plants under laboratory and greenhouse conditions. HR provides a rapid detection tool, requires limited sample preparation and is a non-invasive technique for plant disease detection (Sankaran *et al*., 2010).

Numerous studies have shown that changes detectable by spectral signature can be diagnostic of specific deviations in plant health status (Liew *et al*., 2008), and specific spectral bands can be used to detect infections before the development of symptoms (West *et al*., 2003; Sankaran *et al*., 2010).

Infections caused by viruses, fungi and bacteria cause significant re-organization of cell metabolism in the early stages of infection, generating specific physical/chemical alterations of the host plants that can be detected through optical spectroscopy (Polischuk *et al*., 1997; Spinelli *et al*., 2004; Naidu *et al*., 2009; Santoro *et al*., 2009; Delalieux *et al*., 2007; Grisham *et al*., 2010; Sankaran *et al*., 2011; Abu-Khalaf, 2015; Lorente *et al*., 2015; Afonso *et al*., 2017).

During our studies aimed at extracting metabolome information from plant material by combined analytical approaches, we have found that spectroscopic knowledge transfer can be driven from techniques giving information on identity and quantity of metabolites to other techniques providing physical information of the samples. In particular, it was found that variability of signals in NMR and mass spectrometry (MS) can be correlated to variability of signals in X-ray diffraction spectra for discrimination of fresh and salt-affected grape leaves, on the basis of cultivars and agronomical practices (Rizzuti *et al*., 2013).

In order to evaluate the potential of spectroscopic knowledge transfer in the detection of plant pathogens we have investigated infections caused by *Ea* on pear plants in a model system, by means of NMR and HR. The goals of this study were: i) to identify possible markers related to *Ea* infection by NMR; and ii) to correlate NMR signals of the identified markers to HR wavelengths with the strongest characters for identification of *Ea* infections.

Materials and methods

Experimental design

Pear plants were examined in the period February-April 2014, in a quarantine greenhouse under controlled conditions (temperature 24°C (±2°C); relative humidity greater than 80%) at CIHEAM, Bari (Italy). Bacterial infections were induced artificially by cut inoculations, using 100 μL of a bacterial suspension (10^8 CFU mL^{-1}). All plants were grown in sterilized growth media and regularly irrigated and fertilized to avoid possible biotic or abiotic stresses.

Three groups of 3-year-old pear plants (*Pyrus communis* cv. Bella di Giugno) were used. One group consisted of four plants inoculated with *Ea*, strain

OMPBO329 (Minardi *et al*., 2003), the second consisted of four plants inoculated with *Pss*, strain CFBP 311 (France), and the third group included four plants which were inoculated with sterilized deionized water and were used as negative controls.

Ten asymptomatic leaves per plant were sampled at three collection times (days post inoculation, dpi): at 0 dpi, just before inoculation (27 Feb 2014), 20 dpi (19 Mar 2014), or 50 dpi (17 Apr 2014). Two collection times, at 20 or 50 dpi, were selected based on symptom expression induced by both pathogens. A total of 40 biological replicates were prepared for each harvesting time and treatment. All harvested samples were coded and stored in plastic bags. Each sample was used for HR measurements and NMR analyses. All plants were inspected daily to monitor the development of symptoms.

HR measurements

HR spectra were acquired by a FieldSpec®3 ASD spectrophotometer (Analytical Spectral Device,) using a specific capture interface formed by an optical fibre connected to the Plant-probe (ASD) "contact" internally illuminated (light source type: halogen bulb, colour temperature: 2,901 K ± 10% and spot size: 10 mm). This proximal sensing system collected real-time hyperspectral reflectance data in the Vis-NIR range between 350–1000 nm (Full Width Half Maximum, FWHM: 3 nm) and SWIR range between 1,000–1,800 nm (FWHM: 10 nm). Spectral channels of the spectroradiometer were sub-sampled and interpolated, providing spectra with a resolution of 1 nm. The acquisition system (plant probe, optical fibre and spectroradiometer) was anchored to a stable workbench to avoid optical absorption noise due to optical fibre motion during measurements. In the greenhouse, asymptomatic leaves were taken from plants and rapidly analysed (upper surface) by the plant probe equipped with a leaf clip. For each run, an internal automatic procedure consisting of calibration and referencing (blank reference and optimization of light) was performed before HR spectrum acquisition. All the acquired HR spectra were stored by the spectroradiometer management software in a proprietary format (asd).

NMR measurements

After HR analysis, pear leaves were washed and freeze-dried at –50°C and 0.045 atm for 24 h in a lyophilizer (Martin-Christ GmbH, Model Alpha 1-4 LSC). Dry leaves were ground using a mortar and pestle, and the resulting powder was sieved (metallic sifter pore size of 0.5 mm) and stored at room temperature under vacuum in a plastic bag protected from light, until analysis. NMR analyses were carried out within 4 months from the harvest.

For each sample, pear leaf powder (25 mg) was added to 1.5 mL of oxalate buffer pH = 4.2 (pH value was reached after addition of 37% HCl to 100 mL of an aqueous solution containing 0.25 M of $Na_2C_2O_4$ and 2.5 10^{-3} M of NaN_3), shaken for 30 min in a Vortex at 2,000 rpm, and centrifuged for 30 min at 4,000 rpm. Extract (0.9 mL) was added to 0.1 mL of 0.15 $\%_w$ of (trimethylsilyl)-propionic-2,2,3,3-d_4 acid sodium salt (TSP) in D_2O. All chemicals were of analytical reagent grade. Hydrochloric acid (37%), sodium oxalate (≥99.5%), deuterium oxide (99%D) and sodium azide (≥99.0%) were obtained from Sigma–Aldrich, and sodium salt of TSP, 99%D) was obtained from Armar Chemicals. Water was double deionised (resistivity: 18 MΩ·cm) with a Milli-Q water purification system (Merck Millipore).

One-dimensional ^{1}H NOESY spectra were recorded on a Bruker Avance I 400 MHz spectrometer equipped with a 5 mm inverse probe and with an autosampler. ^{1}H NOESY spectra were acquired with 128 scans of 64K data points with a spectral width of 8,013 Hz, a pulse angle of 90°, an acquisition time of 4.09 s, a mixing time of 10 ms and a recycle delay of 3.0 s. Each spectrum was acquired using TOPSPIN 3.0 software (Bruker BioSpin GmbH) under an automatic procedure lasting approx. 22 min, and consisting of sample loadings, temperature stabilization for 5 min, tuning, matching, shimming and 90° pulse calibration. Free induction decays (FIDs) were Fourier transformed, the phase was manually corrected, the baseline was automatically corrected and the spectra were aligned by setting the TSP singlet to 0 ppm. Signal attribution was made by comparison with spectra of authentic samples and with literature data (Ali *et al*., 2011; Ferrara *et al*., 2013, 2014; Rizzuti *et al*., 2013, 2015; Gallo *et al*., 2014). The levels of chemical identification were in accordance with the published guidelines for metabolomics studies (Salek *et al*., 2013).

NMR spectra were converted in regular rectangular buckets (0.04 ppm width) in the range between 8.5 and 0.5 ppm by AMIX 3.9.13. Principal Component Analysis (PCA) was performed using AMIX 3.9.13 software (Bruker BioSpin GmbH).

Pre-processing of HR data

Raw spectral data from pear leaves were pre-processed, eliminating irregular and distorted spectral curves by ViewSpecPro® ASD software. The resulting data were then exported as text format (American Standard Code for Information Interchange, ASCII) and imported in a Matlab routine R2011b (MathWorks, Inc.) developed by the authors for further correction and filtering. "Noisy bands" of the UV region from 350 nm to 400 nm were truncated and the interval ranging between 400 nm and 1,800 nm was considered as HR spectra. In all remaining bands a smoothing filter Savitzky-Golay with frame size of 15 data points (2nd Degree polynomial) was applied (Nevius and Pardue, 1984). Chemometric analyses were performed by STATISTICA 8 software (StatSoft, Inc.).

Pre-processing of NMR data

NMR spectra were converted in regular rectangular buckets (0.04 ppm width) in the range between 8.5 and 0.5 ppm by AMIX 3.9.13. Chemometric analyses were performed by means of AMIX 3.9.13 software (Bruker BioSpin GmbH).

Principal Component Analysis

Principal Component Analysis (PCA) is a multivariate unsupervised statistical method that reduces the dimensionality of data to a subspace, consisting in a few principal components (PCs) which are related to directions of largest amount of the variance in the spectra matrix. Results of PCA are presented as scores and loadings in the corresponding plots. Each spectrum (and then each leaf sample) is represented by a data point in the *scores* plot. Samples characterized by similar spectral features are grouped in the *scores* plot. In the *loadings* plots, variables (rectangular buckets) are identified which are responsible for grouping of the sample.

Covariance analysis

The correlations between NMR and HR data vectors were studied by calculating the covariance matrix:

$$COV_{AB}(i,j) = \sum_k \left(\hat{y}_k(i) - \langle \hat{y}(i) \rangle\right)_A \left(\hat{y}_k(j) - \langle \hat{y}(j) \rangle\right)_B$$

where A and B stand for NMR and HR, respectively, $\hat{y}_k(i)$ is the bucket of sample k and $\langle \hat{y}(i) \rangle$ is the average value calculated over the samples for the i-th variable. Calculation of the covariance matrix was performed using RootProf software (Caliandro and Belviso, 2014).

Results and discussion

Symptom development

Symptoms of fire blight caused by *Ea* became increasingly apparent, and after 20 dpi some leaves and stems of *Ea*-inoculated plants were completely necrotic. All leaves of plants inoculated with *Pss* were asymptomatic after 20 dpi, and necrosis was evident about 50 dpi. However, all plants used as controls maintained optimum vegetative vigour status up to 50 dpi, when the last measurement was carried out. Only asymptomatic leaves were selected for HR and NMR analyses at the three observation times (0, 20 or 50 dpi).

HR analyses

Figure 1 shows the reflectance curves in the range 400-1,800 nm of spectra from typical control leaves at 0 dpi, 20 dpi and 50 dpi. Qualitatively, the curves show the effects of natural growth of the leaves on the reflectance bands. In the 400–700 nm region, the inten-

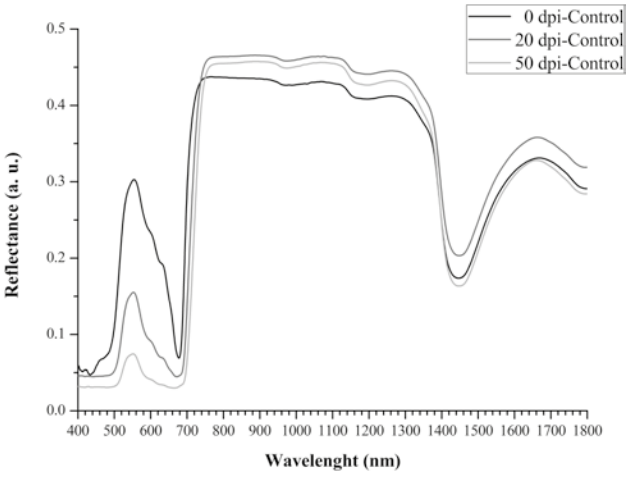

Figure 1. Typical HR spectra for pear leaf samples from 0 dpi-control, 20 dpi-control and 50 dpi-control pear leaves samples.

sity of the bands decreased with time. In this region, bands at 450–495 nm and at 620–700 nm were ascribable to the presence, respectively, of chlorophylls a and b (Ben-Dor *et al.*, 1997; Thenkabail *et al.*, 2014). Leaves at 0 dpi resulted in greater values of reflectance in the green region (510–600 nm) when compared to leaves at 20 dpi or 50 dpi. This can be ascribed to lower concentrations of chloroplasts (chlorophylls, carotenoids) in leaves that were not fully mature. In the region between 680 and 730 nm, reflection increased to values ranging from 43 to 46 % of the total reflectance, depending on the maturity stages of the leaves. Leaf maturity also affects the region between 800 and 1,300 nm (near and medium infrared plateau). In particular, curve sections between 800 and 900 nm were characterized by negative slopes for juvenile conditions, null slopes for almost adult conditions and positive slopes for mature leaves. Furthermore, curve sections between 800 and 1300 nm showed greater reflectance for leaves collected at 20 dpi and 50 dpi than those at 0 dpi. This may be due to greater light scattering from adult leaves (richer in lignocellulosic compounds, structurally more reflecting) compared with young leaves.

To provide an overall perspective of the samples, PCA was applied to HR spectral data, to evaluate effects of leaf age and inoculation on HR spectral features. The qualitative spectroscopic changes due to leaf age were confirmed by PCA, but, overall, these changes were not significant for discrimination of the three group samples (0, 20 or 50 dpi), as shown in Figure S1. Conversely, inoculations affected sample distribution in PC1/PC2 *scores* plot. Figure 2 shows the PC1/PC2 *scores* plot for leaf samples (pathogen inoculated and controls) after 20 dpi. A clear discrimination between *Ea* (positive values of PC1) and control (negative values of PC1) was obvious along PC1which explains 93.3% of the total variance. HR spectral features from the *Pss*-inoculated leaves resembled those from the control samples. After 50 dpi, differentiation of the *Ea*-inoculated group from the other clusters was also apparent along PC1 (Figure S2), although the explained variance decreased to 60.3%. Leaves from the *Pss*-inoculated samples could be distinguished from control and *Ea* samples.

Interpretation of the corresponding 1D *loadings* plots (Supporting information: Section S1, Figures S3 S4) permitted identification of wavelength values responsible for the "spontaneous groupings" found among the three inoculation treatments. Table S1 summarizes these wavelength values as functions of leaf age (dpi), inoculation treatments (control, *Ea* or *Pss*), and biochemical/biophysical absorption characteristics.

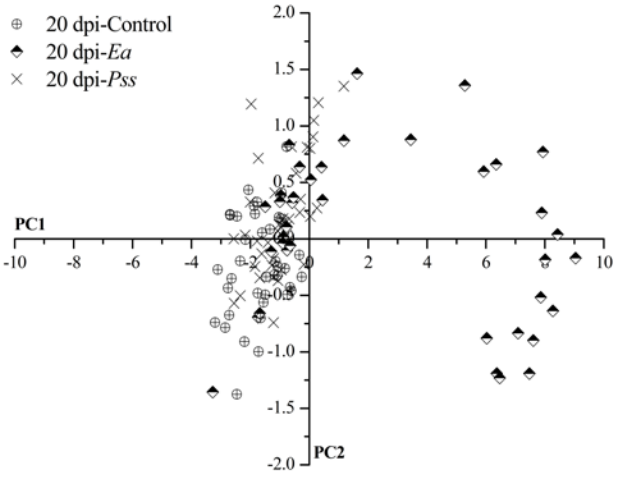

Figure 2. PC1/PC2 *scores* plot obtained after PCA applied to HR data for pear leaf samples from 20 dpi-control, 20 dpi-*Ea* and 20dpi-*Pss* treatments.

NMR analyses

A typical ^{1}H-NMR spectrum of a pear leaf sample is shown in Figure 3. The ^{1}H-NMR spectra can be divided into three regions:

a) The region between 10.00 ppm and 5.50 ppm showed weak signals attributable to phenolic and other aromatic compounds. Doublets at 6.41 ppm and 7.66 ppm were attributed to the olefinic protons of chlorogenic acid; the aromatic protons of the chlorogenic acids were found at 7.21 ppm, 7.14 ppm and 6.96 ppm. Four singlets at 8.42 ppm, 7.09 ppm, 6.81 ppm and 6.56 ppm were ascribed, respectively, to formic acid, gallic acid, hydroquinone and fumaric acid. Two signals at 6.99 ppm and 6.86 ppm due to the aromatic protons of the 6-O-acetylarbutin were also identified;

b) The region from 5.50 ppm to 3.00 ppm mainly contained sugar signals. Peaks attributable to sorbitol were found at 3.84 ppm, 3.82 ppm, 3.72 ppm and 3.65 ppm. Anomeric protons of sucrose, α- and β-glucose appeared, respectively, at 5.40 ppm, 5.23 ppm and 4.64 ppm. In this region the singlet at 3.19 ppm, ascribable to the choline, and other signals due to metabolites

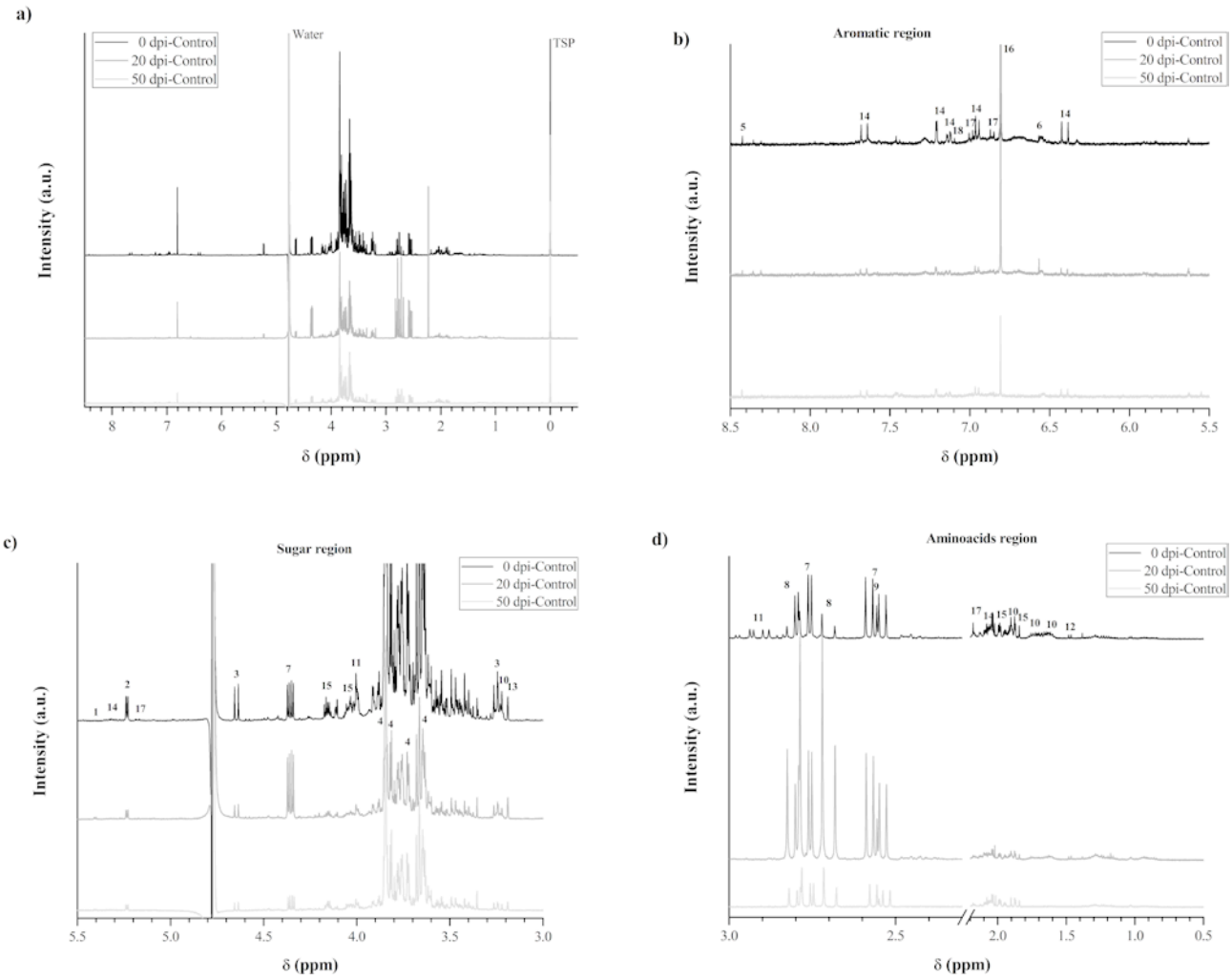

Figure 3. Typical ^{1}H-NMR spectrum of a pear leaf sample. a) the full ^{1}H-NMR spectrum is divided into three regions: b) aromatic regions, c) sugar region and d) aminoacid region. Peak labels assigned according to Table 1.

such as chlorogenic acid (5.32 ppm, 4.25 ppm and 3.88 ppm), 6-O-acetylarbutin (5.18 ppm), malic acid (4.35 ppm), quinic acid (4.16 ppm and 4.03 ppm) and arginine (3.23 ppm), were also observed;

c) In the region from 3.00 ppm to 0.50 ppm, signals were present for amino acids such as asparagine (2.93 ppm), arginine (1.75 ppm and 1.62 ppm) and alanine (1.47 ppm), as well as for organic acids such as citric acid (2.80 ppm and 2.70 ppm), malic acid (2.77 ppm and 2.57 ppm), succinic acid (2.56 ppm), and quinic acid (2.08 ppm, 2.06 ppm, 1.96 ppm and 1.87 ppm).

The metabolites identified by ^{1}H NMR are listed in Table S2.

As described above for HR data, NMR spectra were also submitted to PCA, to evaluate possible effects of leaf age and inoculation on NMR spectral features. PCA of NMR spectra of the control samples at 0, 20 or 50 dpi was performed. The PC1/PC2 *scores* plot in Figure S5 showed that the samples were grouped depending on the harvesting time (0 dpi, 20 dpi or 50 dpi). Along PC1, which explained 56.2 % of the total variance, 0 dpi control samples were at positive scores and were clearly separated from the 20 dpi-control and 50 dpi-control samples, which had negative scores. Along PC2, which explains 13.6 % of the total variance, the 20 dpi-control samples were

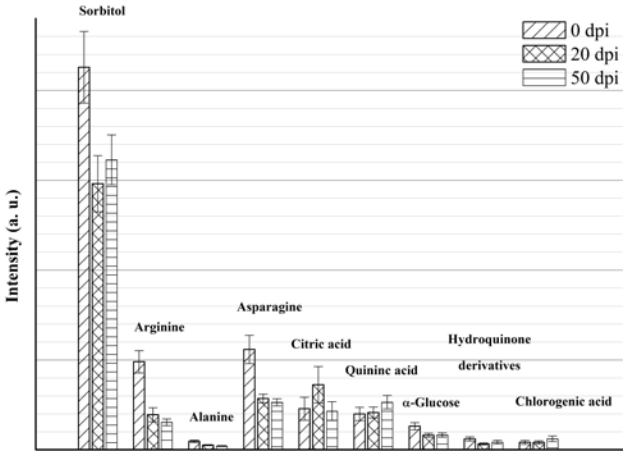

Figure 4. NMR signal distribution of selected metabolites at for pear leaf samples from 0 dpi, 20 dpi and 50 dpi treatments.

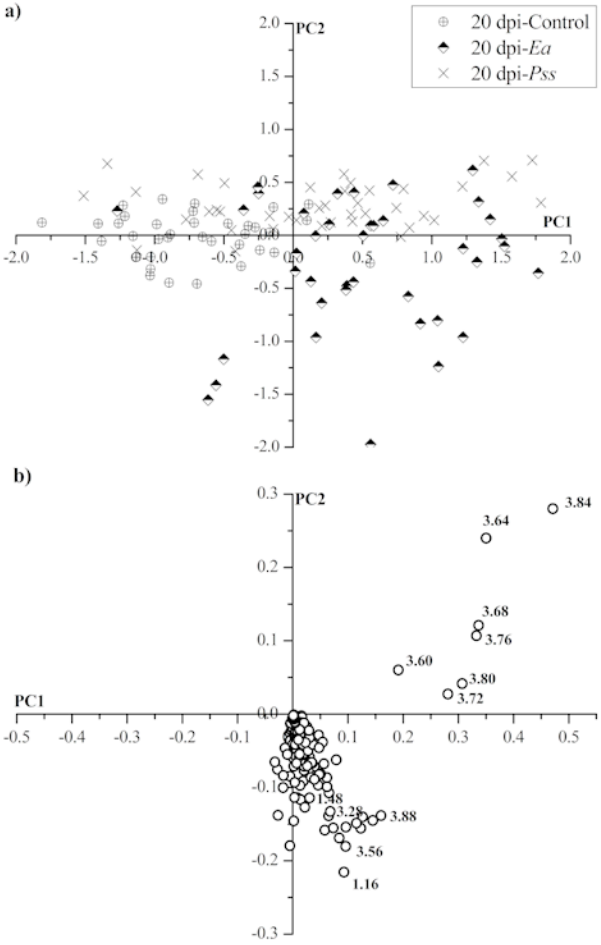

Figure 5. a) PC1/PC2 *scores* plot and b) PC1/PC2 *loadings* plot obtained after PCA applied to NMR data for pear leaf samples from 20 dpi-control, 20 dpi-*Ea* and 20 dpi-*Pss* treatments.

differentiated from the 50 dpi samples. Among the signals responsible for this differentiation, those at 3.84, 3.64, 3.68, 3.76, 3.80 and 3.72 ppm, ascribed to sorbitol, decreased during plant growth from 0 dpi to 50 dpi. The amino acids arginine (3.24 and 1.92 ppm), asparagine (4.00 ppm) and alanine (1.47 ppm) were also of reduced concentrations after 50 d. In contrast, the contents of quinic acid (4.16, 2.04 and 2.00 ppm) increased during the plant growth. Signals at 2.80, 2.72, 2.68 ppm for citric acid characterized the 20 dpi-control samples. Their intensity increased during the first 20 d and returned to the initial values after further 30 d. PCA carried out using buckets from the region between 8.50 and 5.10 ppm (Figure S6) indicated that signal intensities of α-glucose (5.24 ppm) and of hydroquinone derivatives (6.80 and 6.86 ppm) decrease during leaf growth, whereas an increase occurred for signals of chlorogenic acid (7.20 and 6.96 ppm).

The distribution of intensities of the NMR signals related to the main metabolites which changed during plant growth is reported in Figure 4. Sorbitol is a polyol which is the primary photosynthetic product, representing 60 to 90% of the carbon exported from leaves towards pear fruits (Hudina *et al.*, 2007). Citric acid is involved in leaf respiration along with carbohydrates (Hudina *et al.*, 2007). Amino acids are used by plants for the synthesis of proteins and have important roles in the nitrogen uptake, assimilation, translocation and remobilization during plant development (Roy *et al.*, 2013). Hydroquinone derivatives have been identified as antibiotic substances associated with fire blight resistance, and are specific markers of pear products for evaluation of product authenticity (Cui *et al.*, 2005). Since hydroquinone and its derivative 6-O-acetyl arbutin are generated by oxidation processes against bacterial invasion, the decrease of their amounts with leaf age is expected when no infections occur, as for the control samples.

Once the effects of the leaf growth on NMR spectral features were accounted for, PCA was applied to NMR data of the control, *Ea* and *Pss* treated leaves collected at 20 dpi. Figure 5 shows PC1/PC2 *scores* and *loadings* plots. Along PC1, which explained 56.1

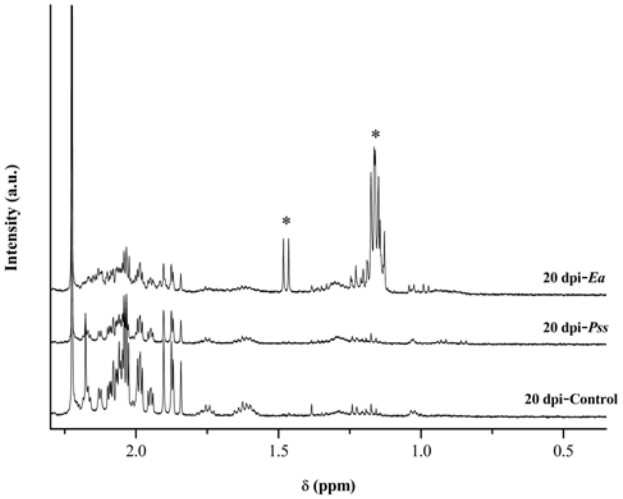

Figure 6. NMR spectra for 20 dpi-*Ea*, 20 dpi-*Pss* and 20 dpi-control pear leaf samples (signals of polysaccharide and alanine are marked with asterisks).

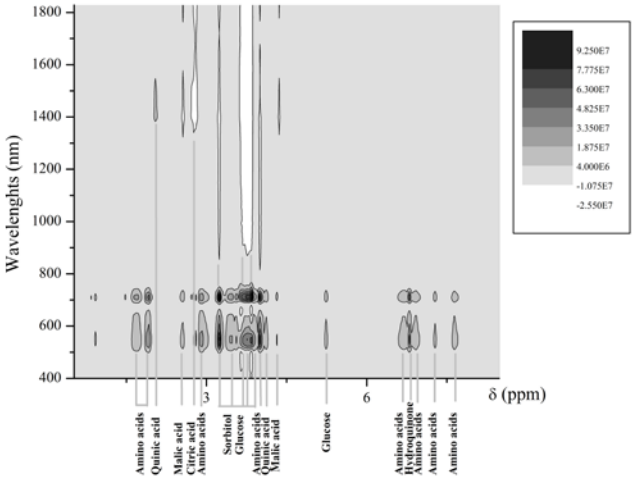

Figure 7. Contour plot resulting from the HR-NMR covariance analysis applied to control pear leaf samples at different plant growth stages.

% of the total variance, *Ea*-inoculated leaves and some of the *Pss*-inoculated leaves were separated from the control leaf samples, and the main signals responsible for this discrimination were those ascribed to sorbitol (between 3.84 and 3.60 ppm). Since sorbitol concentrations decrease during plant growth, greater amounts in infected leaves at 20 dpi indicates reduced consumption of this sugar, due to a particular stress condition. NMR spectra of *Ea*-inoculated samples were characterized by the presence of two signals: a doublet at 1.47 ppm and a multiplet at 1.16 ppm (Figure 6). The first belongs to the methyl protons of alanine, while the second was ascribed to a methyl group of a fucosyl residue of a polysaccharide (or lipopolysaccharide). Formation of these compounds is triggered by *Ea* infection (Ray *et al.*, 1987; Vrancken *et al.*, 2013). In Figure S7, the distribution of the intensities of the signal at 1.16 ppm is outlined for all of the 20 dpi leaf samples.

Statistical analyses applied to NMR data of the control, *Ea* and *Pss* samples at 50 dpi indicated that the signal at 1.16 ppm was still present in some *Ea*-inoculated leaves (Figure S8), although the number of samples marked by the fucosyl group was less than that found at 20 dpi. The fucosyl residue of the polysaccharide (or lipopolysaccharide) was therefore confirmed as the strongest discriminating factor of *Ea* infections compared to *Pss* infections.

HR-NMR covariance analyses

A covariance matrix results in a normal 2D spectrum containing crosspeaks relating the data of the two evaluation techniques. These cross-peaks indicate correlated fluctuations of intensity throughout the ensemble of underlying spectra. Cross-peaks are positive when fluctuations have the same sign, and are negative when fluctuations have opposite sign. Signals arising from the same molecule are positively correlated.

The contour plot resulting from the HR-NMR covariance analyses applied to control leaf samples at different plant growth stages (Figure 7) indicated consumption of sorbitol, amino acids and hydroquinone which can be monitored by analysing the bands at 540 nm and 710 nm of the HR spectrum. HR bands centred at 540 nm and 710 nm were positively correlated with the NMR peaks ascribable to sorbitol and glucose (3.24–3.84 ppm, 5.23 ppm), amino acids (1.75 ppm, 1.92 ppm, 2.93, 4.01 ppm, 6.7 ppm, 6.9 ppm, 7.3 ppm, 7.6 ppm), and hydroquinone (6.81 ppm). HR band ranging between 1,380 and 1,520 nm was positively related to the NMR signal at 2.06 ppm, ascribed to quinic acid, and negatively correlated with the NMR signal at 2.80 ppm, ascribed to citric acid. HR bands between 900 and 1,800 nm were strongly inversely correlated to the sorbitol content. The negative sign of this correlation indicates that decreased sorbitol during the plant growth corresponded to

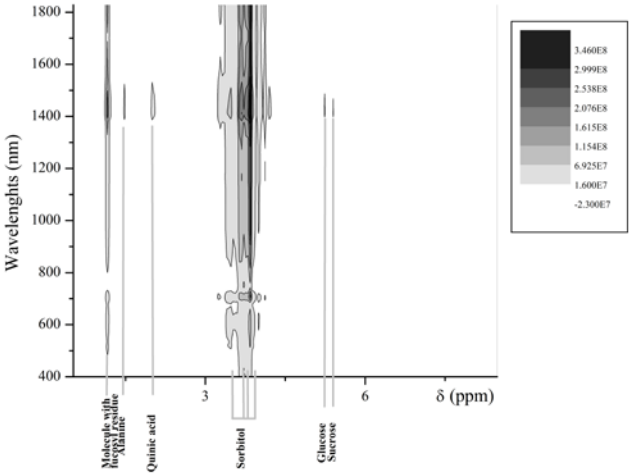

Figure 8. Contour plot resulting from the HR-NMR covariance analysis applied data for pear leaf samples from control, *Ea and Pss* treatments. Samples harvested at 20 dpi.

increases of the 900–1,800 nm reflectance in the HR spectra of the control leaves.

The contour plot resulting from the HR-NMR covariance analysis applied to control, *Ea* and *Pss* samples harvested at 20 dpi (Figure 8) showed positive correlation between sugars such as sorbitol (3.65–3.84 ppm), glucose (5.23 ppm) and sucrose (5.40 ppm) and the band centred at 1,400 nm. The HR band at 1,400 nm also correlated positively to the NMR signals of two metabolites characterizing the *Ea* inoculated leaf samples, i.e. the molecule with a fucosyl residue at 1.16 ppm and alanine (1.47 ppm). This correlation can be attributed to infection of the leaves for the *Ea* and *Pss* inoculated samples.

At 50 dpi, HR-NMR covariance analyses applied to control, *Ea* and *Pss* leaves (Table 1) showed positive correlation between HR bands centred at 850 nm and 1,050 nm, and the NMR signal of the fucosyl moiety at 1.16 ppm, which was the marker for the *Ea*-inoculated samples.

The only previous study that aimed to detect fire blight by spectroscopy (NIR spectroscopy) under controlled conditions was that reported by Spinelli *et al.* (2004). They suggested that NIR analysis did not allow early diagnosis of the disease, due to the limited leaf observation surface (spots of about 2 mm^2). In contrast, our combined HR/NMR approach revealed the possibility to link specific regions of the HR spectrum to markers of the infection by *Ea*. This approach also

Table 1. NMR-HR covariance correlations for pear leaves sampled at 50 dpi.

Metabolite	NMR signal (ppm)	HR band (nm)	Correlation
Sorbitol	3.65-3.84	1400	Negative
Citric acid	2.70 and 2.80	740	Positive
Quinic acid	2.06	900-1400	Negative
Hydroquinone	6.81	900-1400	Negative
Molecule having a fucosyl residue	1.16	850 1050	Positive Positive

permitted detection of infections at 20 dpi. The reason for the different results obtained in the present study and those of Spinelli *et al.* (2004) may be *i*) the different observation times used in the two studies; *ii*) the different detection leaf area (2 mm^2 at 650–1200 nm *versus* 314 mm^2 at 400–1830 nm); *iii*) the characteristics of the inoculated bacterial strains; *iv*) the susceptibility of the pear variety used (cv. Bella di Giugno *vs* cv. Abbé Fétél); and/or *v)* the methodological and instrumental conditions in which spectra were acquired (e.g. direct or indirect contact of leaves, lighting conditions).

In conclusion, NMR analyses of pear leaves indicates that, depending on the detection period, alanine and a fucosyl-containing polysaccharide are the metabolites mainly associated with infections by *Ea*. Using NMR-HR covariance analyses, HR bands correlated to these metabolites were identified. After 20 d from inoculation, the HR band at 1,400 nm correlated positively to the NMR signals for alanine and a polysaccharide containing the fucosyl residue. After 50 d, bands centred at 850 nm and 1,050 nm were positively correlated to the fucosyl group, which can be considered a marker for the *Ea* infected pear leaf samples.

The spectroscopic knowledge transfer approach used in this study gave NMR-HR maps representing the specific infection status of pear plants. This result could facilitate development of methods and handheld optical devices for the detection of *Ea* infections in pear plants.

Conflict of interest

The authors declare that they have no conflicts of interest.

Acknowledgements

Yaseen Alnaasan supported this research with spectral acquisitions and Elvira Lapedota assisted with English language revision of the manuscript of this paper.

Literature cited

Abu-Kalaf M., 2015. Sensing tomato's pathogen using Visible/Near infrared (VIS/NIR) spectroscopy and multivariate data analysis (MVDA). *Palestine Technical University Research Journal* 3, 12–22.

Afonso A.M., R. Guerra, A.M. Cavaco, P. Pinto, A. Andrade, A. Duarte, D.M. Power and N.T. Marques, 2017. Identification of asymptomatic plants infected with Citrus tristeza virus from a time series of leaf spectral characteristics. *Computers and Electronics in Agriculture* 141, 340–350.

Ali K., F. Maltese, A.M. Fortes, M.S. Pais, Y.H. Choi and R. Verpoorte, 2011. Monitoring biochemical changes during grape berry development in Portuguese cultivars by NMR spectroscopy. *Food Chemistry* 124, 1760–1769.

Ben-Dor E., Y. Inbar and Y. Chen, 1997. The reflectance spectra of organic matter in the visible near-infrared and short wave infrared region (400–2500 nm) during a controlled decomposition process. *Remote Sensing of Environment* 61, 1–15.

Bevilacqua V., M. Triggiani, V. Gallo, I. Cafagna, P. Mastrorilli and G. Ferrara, 2012. An Expert System for an Innovative Discrimination Tool of Commercial Table Grapes. In: *Intelligent Computing Theories and Applications. ICIC 2012. Lecture Notes in Computer Science* (D.-S. Huang, J. Ma, K.-H. Jo, M.M. Gromiha, ed.), Springer, Berlin, Heidelberg, 95–102.

Billing E., 2000. Fire blight risk assessment systems and models. In: *Fire Blight: The Disease and Its Causative Agent, Erwinia amylovora* (J.L. Vanneste, ed.), CAB International, Wallingford, UK, 293–318.

Bonn W.G. and T. van der Zwet, 2000. Distribution and economic importance of fire blight. In: *Fire Blight: The Disease and Its Causative Agent, Erwinia amylovora* (J.L. Vanneste, ed.), CAB International, Wallingford, UK, 37–53.

Caliandro R., and D.B. Belviso, 2014. RootProf: software for multivariate analysis of unidimensional profiles. *Journal of Applied Crystallography* 47, 1087–1096.

Choi Y.H., E.C. Tapias, H.K. Kim, A.W.M. Lefeber, C. Erkelens, J.T.J. Verhoeven, J. Brzin, J. Zel and R. Verpoorte, 2004. Metabolic discrimination of *Catharanthus roseus* leaves infected by Phytoplasma using ^{1}H-NMR spectroscopy and multivariate data analysis. *Plant Physiology* 135, 2398–2410.

Cui T., K. Nakamura, L. Ma, J.-Z. Li and H. Kayahara, 2005. Analyses of arbutin and chlorogenic acid, the major phenolic constituents in oriental pear. *Journal of Agricultural and Food Chemistry* 53, 3882–3887.

Delalieux S., J. Van Aardt, W. Keulemans, E. Schrevens and P. Coppin, 2007. Detection of biotic stress (*Venturia inaequalis*) in apple trees using hyperspectral data: Non-parametric statistical approaches and physiological implications. *European Journal of Agronomy* 27, 130–143.

Ferrara G., A. Mazzeo, A.M.S. Matarrese, C. Pacucci, A. Pacifico, G. Gambacorta, M. Faccia, A. Trani, V. Gallo, I. Cafagna and P. Mastrorilli, 2013. Application of abscisic acid (S-ABA) to "Crimson Seedless" grape berries in a mediterranean climate: effects on color, chemical characteristics, metabolic profile, and S-ABA concentration. *Journal of Plant Growth Regulation* 32, 491–505.

Ferrara G., A. Mazzeo, G. Netti, C. Pacucci, A.M.S. Matarrese, I. Cafagna, P. Mastrorilli, M. Vezzoso and V. Gallo, 2014. Girdling, Gibberellic Acid, and Forchlorfenuron: Effects on yield, quality, and metabolic profile of table grape cv. Italia. *American Journal of Enology and Viticulture* 65, 381–387.

Gallo V., P. Mastrorilli, I. Cafagna, G.I. Nitti, M. Latronico, F. Longobardi, A.P. Minoja, C. Napoli, V.A. Romito, H. Schäfer, B. Schütz and M. Spraul, 2014. Effects of agronomical practices on chemical composition of table grapes evaluated by NMR spectroscopy. *Journal of Food Composition and Analysis* 35, 44–52.

Grisham M.P., R.M. Johnson and P.V. Zimba, 2010. Detecting Sugarcane yellow leaf virus infection in asymptomatic leaves with hyperspectral remote sensing and associated leaf pigment changes. *Journal of virological methods*, 167, 140–145.

Hudina M., M. Colarič and F. Štampar, 2007. Primary metabolites in the leaves and fruits of three pear cultivars during the growing season. *Canadian Journal of Plant Science* 87, 327–332.

Jacquart-Romon C. and J.P. Paulin, 1991. A computerized warning system for fire blight control. *Agronomie* 11, 511–519.

Leiss K.A., Y.H. Choi, R. Verpoorte and P.G.L. Klinkhamer, 2011. An overview of NMR-based metabolomics to identify secondary plant compounds involved in host plant resistance. *Phytochemistry Reviews* 10, 205–216.

Liew O.W., P.C.J. Chong, B. Li and A.K. Asundi, 2008. Signature optical cues: emerging technologies for monitoring plant health. *Sensors* 8, 3205–3239.

Lima M.R.M., M.L. Felgueiras, G. Graça, J.E. Rodrigues, A. Barros, A.M. Gil and A.C. Dias, 2010. NMR metabolomics of esca disease-affected *Vitis vinifera* cv. Alvarinho leaves. *Journal of Experimental Botany* 61, 4033–4042.

Longobardi F., A. Ventrella, A. Bianco, L. Catucci, I. Cafagna, V. Gallo, P. Mastrorilli and A. Agostiano, 2013. Non-targeted ^{1}H NMR fingerprinting and multivariate statistical analyses for the characterisation of the geographical origin of Italian sweet cherries. *Food Chemistry* 141, 3028–3033.

Lorente D., P. Escandell-Montero, S. Cubero, J. Gómez-Sanchis and J. Blasco, 2015. Visible–NIR reflectance spectroscopy and manifold learning methods applied to the detection of fungal infections on citrus fruit. *Journal of Food Engineering* 163, 17–24.

Minardi P., M. Morbio, F. Traversa and U. Mazzucchi, 2003. Variabilità genomica di ceppi di *Erwinia amylovora* associati a infezioni su piante ospiti diverse. *Notiziario Tecnico* 66, 38–44.

Naidu R. A., E.M. Perry, F.J. Pierce and T. Mekuria, 2009. The potential of spectral reflectance technique for the detection of Grapevine leafroll-associated virus-3 in two red-berried wine grape cultivars. *Computers and Electronics in Agriculture* 66, 38–45.

Nevius T.A. and H. Pardue, 1984. Development and preliminary evaluation of modified Savitzky-Golay smoothing functions. *Analytical Chemistry* 56, 2249–2251.

Nicholson J.K. and J.C. Lindon, 2008. Systems biology: Metabonomics. *Nature* 455, 1054–1056.

Polischuk V.P., T.M. Shadchina, T.I. Kompanetz, I.G. Budzanivskaya, A.L. Boyko and A.A. Sozinov, 1997. Changes in reflectance spectrum characteristic of Nicotiana debneyi plant under the influence of viral infection. *Archives of Phytopathology and Plant Protection* 31, 115–119.

Ray T.C., A.R.W. Smith, R. Wait and R.C. Hignett, 1987. Structure of the side chain of lipopolysaccharide from Erwinia amylovora T. *European Journal of Biochemistry* 170, 357–361.

Rizzuti A., R. Caliandro, V. Gallo, P. Mastrorilli, G. Chita and M. Latronico, 2013. A combined approach for characterisation of fresh and brined vine leaves by X-ray powder diffraction, NMR spectroscopy and direct infusion high resolution mass spectrometry. *Food Chemistry* 141, 1908–1915.

Rizzuti A., L.M. Aguilera-Sáez, V. Gallo, I. Cafagna, P. Mastrorilli, M. Latronico, A. Pacifico, A.M.S. Matarrese and G. Ferrara, 2015. On the use of Ethephon as abscising agent in cv. Crimson Seedless table grape production: Combination of Fruit Detachment Force, Fruit Drop and metabolomics. *Food Chemistry* 171, 341–350.

Roy N., S. Laskar and A. Barik, 2013. Amino acids through developmental stages of sunflower leaves. *Acta Botanica Croatica* 72, 23–33.

Salek R.M., C. Steinbeck, M.R. Viant, R. Goodacre and W.B. Dunn, 2013. The role of reporting standards for metabolite annotation and identification in metabolomic studies. *GigaScience* 2, 13.

Sankaran S., A. Mishra, R. Ehsani and C. Davis, 2010. A review of advanced techniques for detecting plant diseases. *Computers and Electronics in Agriculture* 72, 1–13.

Sankaran S. and R. Ehsani, 2011. Visible-near infrared spectroscopy based citrus greening detection: Evaluation of spectral feature extraction techniques. *Crop Protection* 11, 1508–1513.

Santoro F, S. Gualano, K. Djelouah, A. Guario and A.M. D'Onghia, 2009. Remote sensing to support the monitoring of Citrus tristeza virus (CTV) infected areas. In: *Citrus tristeza virus and Toxoptera citricidus: A serious threat to the Mediterranean citrus industry* (A.M. D'Onghia, K. Djelouah, C.N. Roistacher, ed.), Bari, CIHEAM, 165-171. (Options Méditerranéennes: Série B. Etudes et Recherches; n. 65).

Spinelli F., M. Noferini and G. Costa, 2004. Near infrared spectroscopy (NIRs): perspective of fire blight detection in asymptomatic plant material. *Acta Horticulturae.* 704, 87–90.

Thenkabail P.S., M.K. Gumma, P. Teluguntla and I.A. Mohammed, 2014. Hyperspectral Remote Sensing of Vegetation and Agricultural Crops. *Photogrammetric Engineering & Remote Sensing (PE&RS)* 80, 697–723.

Thomson S.V., 2000. Epidemiology of fire blight. In: *Fire Blight: The Disease and Its Causative Agent, Erwinia amylovora* (J.L. Vanneste, ed.),CAB International, Wallingford, UK, 9–36.

van der Zwet T. and S.V. Beer, 1995. *Fire blight: its nature, prevention, and control: a practical guide to integrated disease management*. United States Department of Agriculture, Series *Agriculture Information Bulletin, no. 631, Washington, D.C.*

Vrancken K., M. Holtappels, H. Schoofs, T. Deckers and R. Valcke, 2013. Pathogenicity and infection strategies of the fire blight pathogen Erwinia amylovora in Rosaceae: State of the art. *Microbiology* 159, 823–832.

West J.S., C. Bravo, R. Oberti, D. Lemaire, D. Moshou and H.A. McCartney, H Alastair, 2003. The potential of optical canopy measurement for targeted control of field crop diseases. *Annual Review of Phytopathology*, 41, 593–614.

Accepted for publication: July 19, 2018